https://doi.org/10.15407/ujpe70.8.516

O.M. KONOVALENKO,[1] Z.A. MAIZELIS [1, 2]

[1] O.Ya. Usikov Institute for Radiophysics and Electronics, Nat. Acad. of Sci. of Ukraine
(Kharkiv 61085, Ukraine)
[2] V.N. Karazin Kharkiv National University
(Kharkiv 61077, Ukraine; e-mail: maizelis.z.a@gmail.com)

MULTIPLE JOINT WEAK MEASUREMENTS AS A WAY TO SUPPRESS THE DECOHERENCE

We apply the multiple, equally spaced in time, weak measurements, to the two-qubit entangled system to decrease the rate of its decoherence, i.e., to prevent the decrease of the off-diagonal elements. The scheme is similar to the Quantum Zeno Effect, but differs by the frequency of the measurements. While the conventional Quantum Zeno Effect assumes rapid measurements which mitigates the Hamiltonian dynamics, the proposed method makes use of entanglement between the qubits to decrease the decoherence rate. We will show that it allows us to partially suppress the decoherence in the case of Lindblad evolution.

K e y w o r d s: joint weak measurements, decoherence suppression, Quantum Zeno Effect, Lindblad evolution.

1. Introduction

Although quantum computing technologies and quantum error correction methods have advanced rapidly, decoherence remains a persistent challenge [1–5]. Unwanted interactions between qubits and external degrees of freedom, such as the electromagnetic modes of experimental setups, induce joint dynamics that transform pure quantum states into mixed states. This non-Hamiltonian behavior can be modeled by quantum kinetic equations [6–8] or through the action of Kraus operators [7, 9].

A variety of strategies have been developed to counteract these deleterious effects. For instance, Quantum Error Correcting Codes [10] protect information by encoding a single logical qubit into an entangled state of several physical qubits, allowing the recovery procedures to be rectified errors introduced by environmental interactions. Alternative methods exploit inherent symmetries to construct decoherence-free subspaces [11] or implement bang-bang (dynamical decoupling) pulses [12–15] to combat noise. However, such pulse sequences are typically limited to countering noise with characteristic frequencies lower than the applied control frequency.

A well-known non-Hamiltonian approach to prevent the unwanted dynamics is provided by the conventional Quantum Zeno Effect (QZE), where repeated strong (projective) measurements "freeze" the evolution of the system, thereby mitigating both decoherence and dissipation [16]. However, the strong back-action of projective measurements can limit flexibility in controlling the system's evolution. In contrast, the method presented here is built upon a series

C i t a t i o n: Konovalenko O.M., Maizelis Z.A. Multiple joint weak measurements as a way to suppress the decoherence. *Ukr. J. Phys.* **70**, No. 8, 516 (2025). https://doi.org/10.15407/ujpe70.8.516.

of weak, equally spaced joint measurements applied to an entangled two-qubit system.

The key innovation in our approach is the use of weak measurements, to decrease the loss of coherence during non-Hamiltonian Lindblad evolution. This brings two principal advantages. First, they allow for a continuous, tunable interaction with the system, enabling an adjustment of the measurement "strength" or influence so that the disturbance can be optimized relative to the system dynamics. Second, unlike the conventional QZE, which requires rapid, strong measurements to halt the system evolution, our strategy operates at measurement frequencies below the thermal bath's characteristic frequencies. This relaxed timing requirement is compensated by tuning the measurement strength, so that the system is gently steered toward the subspace corresponding to the prescribed entangled states dictated by the quantum algorithm.

Many conventional methods focus on protecting individual qubits or using the symmetry of noise to form decoherence-free subspaces. However, in many quantum algorithms the qubits are inherently entangled in predetermined configurations. By using prior knowledge of these allowed entangled states, our method actively suppresses decoherence through joint measurements that project the overall state onto the desired entangled subspace. This flexible control, implemented within the framework of Lindblad evolution, not only reduces decoherence but also preserves the crucial entanglement between qubits more effectively than conventional strong measurement techniques.

The paper is organized as follows. In Section 2, we review the principles of the conventional Quantum Zeno Effect and detail our proposed method for decoherence suppression via joint weak measurements. Section 3 demonstrates the application of this method to a two-qubit system and provides both numerical results and analytic asymptotic relations to analyze the effectiveness of preserving the entanglement. Section 3.3 investigates how the method efficiency depends on key system parameters, such as measurement frequency, decoherence rate, and the system initial state, with special emphasis on the tunability afforded by the weak measurement approach. Finally, Section 4 summarizes the results and discusses potential applications in quantum algorithm design, where the exploitation of predetermined entangled configurations offers a promising route to mitigate decoherence.

2. Method for Suppression of Decoherence

2.1. Freezing of unitary evolution

In contrast to the conventional Quantum Zeno Effect (QZE) based on strong (projective) measurements, our method continuously and gently guides the system state toward a pre-selected subspace. This subspace is determined by the allowed entangled states known from the quantum algorithm. Instead of an regular collapse, weak measurements exert a backaction that can be tuned to balance the interplay between the unitary dynamics and decoherence induced by the environment.

Traditionally, the QZE is illustrated by starting with an initial state $|\Psi_0\rangle$ that evolves under a time-independent Hamiltonian $\mathcal{H}$. In the projective case, after each interval Δt, the state is fully projected back onto $|\Psi_0\rangle$ according to

$$\rho_t = \frac{\left(P\, e^{-i\mathcal{H}\Delta t}\right)^N P\,|\Psi_0\rangle\langle\Psi_0|\,P\left(e^{i\mathcal{H}\Delta t}\,P\right)^N}{Tr\left[\left(P\, e^{-i\mathcal{H}\Delta t}\right)^N P\,|\Psi_0\rangle\langle\Psi_0|\,P\left(e^{i\mathcal{H}\Delta t}\,P\right)^N\right]},$$

with the projector $P = |\Psi_0\rangle\langle\Psi_0|$ and $N+1$ number of projections. This result can be easily obtained by subsequent applycation by Hamiltonian propagator and projector P to the initial state $\rho_0 = |\Psi_0\rangle\langle\Psi_0|$. A short-time expansion of the evolution operator, $e^{-i\mathcal{H}\Delta t} \approx 1 - i\mathcal{H}\Delta t - \frac{1}{2}\mathcal{H}^2\Delta t^2$, shows that the survival probability

$$p(\Delta t) = \left|\langle\Psi_0|e^{-i\mathcal{H}\Delta t}|\Psi_0\rangle\right|^2, \tag{1}$$

deviates from unity only quadratically in Δt. Thus, in the limit of rapid projective measurements the state appears "frozen" with respect to the unitary dynamics.

However, when the system interacts with an environment, its evolution becomes non-Hamiltonian. Such effects are commonly modeled by Lindblad equation with Liouvillian $\mathcal{L}$:

$$\dot\rho = \mathcal{L}\rho = -i[\mathcal{H},\rho] + \sum_i \left(L_i\,\rho\,L_i^\dagger - \frac{1}{2}\{L_i^\dagger L_i,\,\rho\}\right). \tag{2}$$

As the initial state, we take the maximally entangled state – the Bell state: $\rho_0 = |\Psi^+\rangle\langle\Psi^+|$, where $|\Psi^+\rangle = \frac{1}{\sqrt{2}}(|00\rangle + \langle 11|)$.

In this situation the additional dissipative terms yield corrections of order Δt (not merely quadratic), and frequent projective measurements do not fully suppress decoherence.

To address this, our approach replaces strong measurements with joint weak measurements that can be applied at frequencies below the thermal bath characteristic rates, while still harnessing the structure of the entangled state space.

2.2. Joint weak measurements for partial decoherence suppression

Rather than projecting the state entirely onto a single initial state, we now consider an evolving algorithm where a subset $\mathcal{S}$ of qubits is known to lie in a specific entangled subspace with basis $\{|\Psi_i\rangle\}$. In our scheme the state preservation is achieved by means of a series of joint weak measurements.

To illustrate this, one may define a set of weak measurement operators $\{M_i\}$ associated with the basis states $|\Psi_i\rangle$. A typical model for a weak measurement operator is

$$M_i = \sqrt{1-q}\, I + \sqrt{q}\, |\Psi_i\rangle\langle\Psi_i|, \tag{3}$$

where q (with $0 < q \ll 1$) quantifies the measurement strength. In the limit $q \to 1$ these operators approach full projective measurements, while for small q they impart only a partial bias toward the desired subspace.

Assuming the system state evolves under the Liouvillian $\mathcal{L}$ for a time interval Δt, the weak measurement update is then expressed as

$$\rho_{t+\Delta t} = \frac{\sum_i M_i\, e^{\mathcal{L}\Delta t}\, \rho_t\, M_i^\dagger}{\mathrm{Tr}\Big(\sum_i M_i\, e^{\mathcal{L}\Delta t}\, \rho_t\, M_i^\dagger\Big)}.$$

Repeating this process $N = t/\Delta t$ times, the cumulative evolution filters out components that do not belong to the allowed entangled subspace, thereby reducing the effective decoherence rate.

This mechanism offers two key advantages. First is a tunable back-action: the parameter q provides control over the measurement-induced disturbance. Unlike projective measurements, weak measurements allow one to balance the perturbation against the natural dynamics of the system. Second, exploiting known entanglement: because the set $\{|\Psi_i\rangle\}$ encodes prior information about valid entangled configurations in the algorithm, the joint weak measurements selectively suppress transitions into states outside this subspace.

In summary, by integrating the non-Hamiltonian dynamics via the Lindblad generator and interleaving it with appropriately tuned joint weak measurements, our method leverages both the slow measurement cadence (relative to the noise frequencies) and the known structure of entanglement among the qubits. This results in a partial, yet effective, suppression of decoherence. While the overall probability of preserving the desired state becomes less than unity, and diminishes with increasing measurement frequency, the flexibility of adjusting q offers a promising route to optimize decoherence control in realistic quantum computing architectures.

3. Preserving the Entanglement in a Two-Qubit System

3.1. Free and measurements-assisted evolution of the system

In this section, we illustrate the weak measurement-assisted protection of entangled states by considering a simple two-qubit system. As before, the qubits, with frequencies ω_1 and ω_2, interact with an external thermal bath that induces decoherence. However, in contrast to the conventional quantum Zeno effect based on projective measurements, we now employ joint weak measurements to gradually steer the system back toward the entangled subspace prescribed by the quantum algorithm.

We begin by considering the uncontrolled evolution. The two qubits are assumed to be initially prepared in a coherent superposition of two Bell states,

$$|\Psi_{\mathrm{in}}\rangle = \frac{\sqrt{p}+\sqrt{1-p}}{\sqrt{2}}\,|01\rangle + \frac{\sqrt{1-p}-\sqrt{p}}{\sqrt{2}}\,|10\rangle.$$

so that for $p = 0$ or $p = 1$ the state is maximally entangled. In many quantum algorithms the proper encoding guides the system to evolve within a known subspace even though the exact state is not predetermined.

The system Hamiltonian is given by

$$\omega_\pm = \frac{\omega_1 \pm \omega_2}{2}, \quad S_z = s_z \otimes I + I \otimes s_z,$$
$$\Delta S_z = s_z \otimes I - I \otimes s_z.$$
$$\mathcal{H} = \omega_+\, S_z + \omega_-\, \Delta S_z.$$

with $s_z = \sigma_z/2$. Decoherence imposed by the thermal bath is modeled within the Lindblad framework. For simplicity, we use a set of Lindblad operators:

$$
\begin{aligned}
&s_{\pm}^{(1)} = s_{\pm} \otimes I, \quad s_{\pm}^{(2)} = I \otimes s_{\pm},\\
&s_{z}^{(1)} = s_{z} \otimes I, \quad s_{z}^{(2)} = I \otimes s_{z}.\\
&L_{2i-1} = \sqrt{\gamma_i\,(\overline{n}+1)}\; s_{-}^{(i)},\\
&L_{2i} = \sqrt{\gamma_i\,\overline{n}}\; s_{+}^{(i)},\\
&L_{4+j} = \sqrt{\gamma_{p\,j}}\; s_{z}^{(j)}, \quad i = 1,2,\ j = 1,2,
\end{aligned}
\tag{4}
$$

where $s_{\pm} = s_x \pm i\, s_y$ and the Planck number $\overline{n}$ (assumed identical for both qubits) characterizes the equilibrium temperature. Operators L_1–L_4 describe the linear energy-exchange interactions with the bath, while L_5 and L_6 model dispersive effects.

In the free evolution, the off-diagonal element ρ_{23} of the density matrix (expressed in the computational basis) evolves as

$$
\rho_{23}^{(\mathrm{free})} \simeq -\frac{1}{2}\left(1 - \frac{A\,t}{2}\right),
$$
$$
A = (2\overline{n}+1)(\gamma_1+\gamma_2) + \gamma_{p1} + \gamma_{p2} + 2\,i\,(\omega_1 - \omega_2).
$$

indicating that both the Hamiltonian dynamics and the linear qubit-bath couplings contribute to decoherence and phase evolution. Figure 1 schematically illustrates the two-qubit setup in contact with the thermal bath.

To counteract decoherence without fully freezing the dynamics, we now introduce a measurement protocol that changes the state toward the desired entangled subspace. In contrast to projective measurements, our approach uses a measurement superoperator $\mathcal{M}$ that induces only partial collapse. In this formulation the measurement update reads

$$
\mathcal{M}[\rho] = (1-q)\,\rho + q \sum_{i=\pm} |\Psi_i\rangle\langle\Psi_i|\,\rho\,|\Psi_i\rangle\langle\Psi_i|,
$$

where the parameter $0 < q \ll 1$ quantifies the measurement strength and the projectors $|\Psi_{\pm}\rangle\langle\Psi_{\pm}|$ select the allowed subspace. After evolving freely for a time interval Δt under the Liouvillian dynamics $e^{\mathcal{L}\Delta t}$, the state is updated as $\rho(t+\Delta t) = \Lambda^{-1}\,\mathcal{M}\big[e^{\mathcal{L}\Delta t}\,\rho(t)\big]$ where $\Lambda = \mathrm{Tr}\big\{\mathcal{M}\big[e^{\mathcal{L}\Delta t}\,\rho(t)\big]\big\}$.

This formulation emphasizes that, at every update, the system undergoes an unperturbed evolution and then a weak projection onto the entangled subspace. By iterating this process, the protocol continuously suppresses deviations from the target state configuration while still allowing for a controlled interplay with the system intrinsic dynamics.

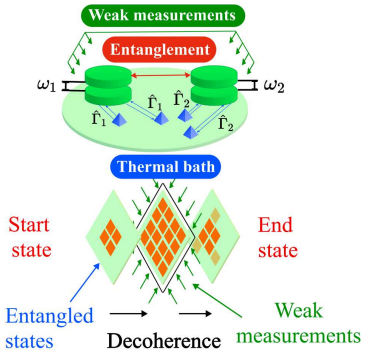

Fig. 1. Schematic representation of a two-qubit system interacting with an external thermal bath. The protocol alternates between periods of Liouvillian evolution and successive joint weak measurements. These measurements project the system state onto the allowed subspace of entangled states (here, the Bell states) in order to suppress decoherence

Under the combined action of the bath and the weak measurements, the contributions arising from Hamiltonian evolution and the linear interactions (proportional to γ_1 and γ_2) are suppressed. For example, the off-diagonal element now evolves approximately as

$$
\rho_{23}^{(\mathrm{meas})} \simeq -\frac{1}{2}\left(1 - \frac{(\gamma_{p1}+\gamma_{p2})\,t}{2}\right).
$$

for $q = 1$, thereby eliminating the dephasing terms due to energy exchange and unitary oscillations. In effect, the joint weak measurements filter out unwanted evolution components while preserving only the dispersive decoherence effects that cannot be compensated by the measurement protocol. This suppression is achieved without requiring a high-frequency projective measurement sequence; the flexibility afforded by tuning the measurement strength q permits the protocol to be applied at intervals that remain compatible with the intrinsic system dynamics.

Figure 2 compares the time evolution of selected density matrix elements under free evolution and under repeated joint weak measurements.

Figure 3 shows the evolution of matrix elements for three different parameters: $q = 0$ (first row, *a*), $q = 0.9$ (second row, *b*), $q = 1$ (third row, *c*), for $\omega_1 t = 0, 10, 20, 30$ (the four columns). The color represents the real part of the matrix elements, with all

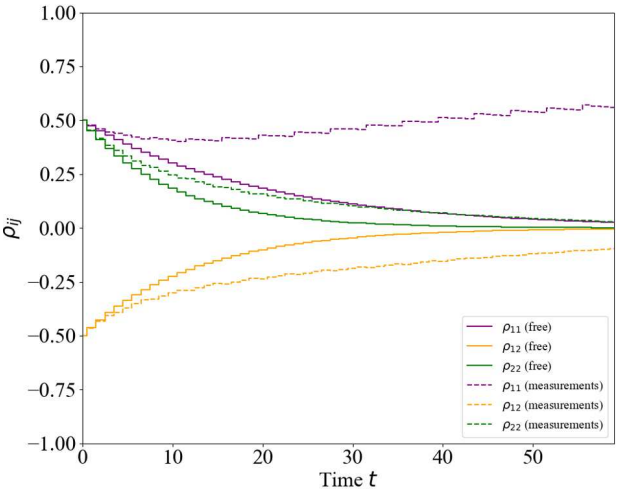

Fig. 2. (Color online) Comparison of the evolution of the density matrix elements in the two-qubit system. The panel shows the time evolution (scaled in units of $1/\omega_1$) of both diagonal and off-diagonal elements under free evolution versus under repeated joint weak measurements. The weak measurement process suppresses contributions from Hamiltonian dynamics and linear qubit-bath couplings, thereby reducing decoherence. Parameters: $\omega_2 = \omega_1$, $\gamma_1/\omega_1 = \gamma_2/\omega_1 = 0.05$, $\gamma_{p1}/\omega_1 = \gamma_{p2}/\omega_1 = = 0.005$, with $N = 50$ measurement updates, and $\overline{n} = 0$

16 elements displayed in each panel. We see as the parameter q increases, the effectiveness of the method increases from first row to the third.

3.2. Characteristics of the effectiveness of the method

To quantify the impact of various parameters on our scheme performance, it is necessary to select measures that reflect the system's coherence. In many cases the coherence is associated with the off-diagonal elements of the density matrix. Among several candidates, including the relative entropy of coherence [17], the Jensen–Shannon divergence [18], and the l_1 norm of quantum coherence [19], we choose the latter. In the computational basis the l_1 norm is defined as

$$C_{l_1} = \sum_{i \neq j} |\rho_{ij}|. \tag{5}$$

In our simple example the contribution to C_{l_1} is dominated by the only initially nonzero off-diagonal element, ρ_{23}.

Decoherence also manifests as a loss of entanglement between qubits. This deterioration can be quantified by several measures, such as the entropy of entanglement [20], negativity [21], and concurrence [22]. Here we employ concurrence, defined by

$$C = \max\left\{0,\ \sqrt{\lambda_1} - \sqrt{\lambda_2} - \sqrt{\lambda_3} - \sqrt{\lambda_4}\right\}, \tag{6}$$

where the λ_i (ordered in decreasing order) are the eigenvalues of the matrix $\rho\,\tilde{\rho}$ with

$$\tilde{\rho} = (\sigma_y \otimes \sigma_y)\,\rho^*\,(\sigma_y \otimes \sigma_y),$$

and ρ^* denotes the complex conjugate of ρ.

Figure 4 shows the time evolution of the concurrence C as given in Eq. (6). It is evident that the rate at which entanglement is lost is substantially reduced, when the weak measurement protocol is applied. In fact, one can compare numerical results with the asymptotic expressions, for small times $t \ll 1/\gamma_{1,2}$, under free decoherence the concurrence decays as

$$C \simeq 1 - t\left[(\gamma_1+\gamma_2)\left(\overline{n}+\tfrac{1}{2}+\sqrt{\overline{n}(\overline{n}+1)}\right)+\tfrac{1}{2}(\gamma_{p1}+\gamma_{p2})\right] \tag{7}$$

whereas, with the measurement protocol with $q = 1$, the decay is given by

$$C \simeq 1 - \frac{t}{2}\sum_{i=1}^{2}\gamma_{pi}. \tag{8}$$

To assess the efficiency of our scheme, we introduce three quantitative characteristics. The first one is defined as

$$\mathcal{E}_{\tan} = \frac{dC_{\text{meas}}}{dt}\left(\frac{dC_{\text{free}}}{dt}\right)^{-1}\Bigg|_{t=0}, \tag{9}$$

which represents the reduction in the instantaneous rate of concurrence decay at $t = 0$. After calculations for an arbitrary initial superposition state Eq. (1), one finds, for $q = 1$,

$$\mathcal{E}_{\tan} = R_m\,(R_f + R_s)^{-1}, \tag{10}$$

where

$$R_m = \gamma_{p1} + \gamma_{p2} + (\gamma_1 - \gamma_2)\sqrt{1-(2p-1)^2},$$
$$R_f = \left(\gamma_{p1} + (2\overline{n}+1)\,\gamma_1\right) + \left(\gamma_{p2} + (2\overline{n}+1)\,\gamma_2\right),$$
$$R_s = \frac{2}{1-2p}\sqrt{\overline{n}(\overline{n}+1)\left[(1-2p)^2(\gamma_1-\gamma_2)^2 + 4\,\gamma_1\gamma_2\right]}.$$

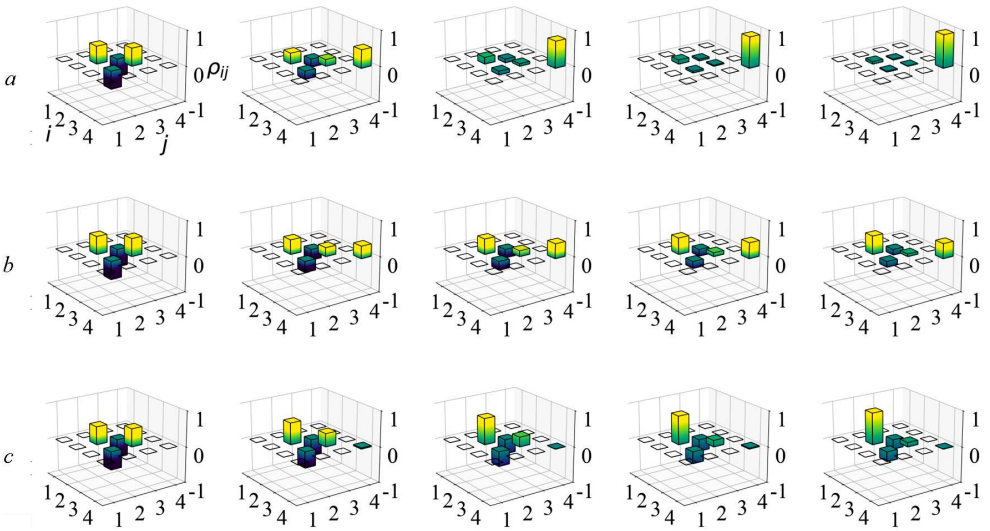

Fig. 3. (Color online) Visual representations of the density matrix ρ at different stages of evolution. Columns corresponds to time moments ($\omega_1 t = 0, 10, 20, 30$): the initial state with no measurement (a); the state after the application of the joint weak measurements with force 0.9 (b); and the state at the same time with force 1 of the joint weak measurements that more efficiently drives the state back onto the desired entangled subspace. Positive matrix elements are depicted in yellow, while negative elements are shown in blue (c)

A second measure of the protocol's efficiency considers the time required for the concurrence to drop to a fixed threshold value (we adopt 0.9 as the criterion). This is given by

$$\mathcal{E}_{\text{time}} = t\big|_{C=0.9,\,\text{free}} \left(t\big|_{C=0.9,\,\text{meas}}\right)^{-1}. \tag{11}$$

Finally, in order to connect the preservation of entanglement with the maintenance of quantum coherence, we compare the decay rates of the l_1 norm coherence measure:

$$\mathcal{E}_{\text{coh}} = \frac{dC_{l_1\text{meas}}}{dt} \cdot \left(\frac{dC_{l_1\text{free}}}{dt}\right)^{-1}\Bigg|_{t=0}. \tag{12}$$

Figure 5 plots all three characteristics as functions of the number of measurement steps executed on a fixed time interval. The similar behavior observed across these metrics confirms that the joint weak measurement protocol effectively preserves both the coherence and the entanglement of the system. In particular, the small steps seen in the $\mathcal{E}_{\text{coh}}(N)$ curve arise from the nonmonotonic nature of $C(t)$ when intersecting with the constant threshold $C_{\text{cr}} = 0.9$. The solid horizontal line in the main panel of Fig. 5 represents the asymptotic value given by Eq. (10). Notably, for moderate measurement frequencies (typically $N \sim 50$ in our example) the protocol achieves its optimal effect, and one can reasonably expect an even greater enhancement in coherence preservation with an increasing number of entangled qubits.

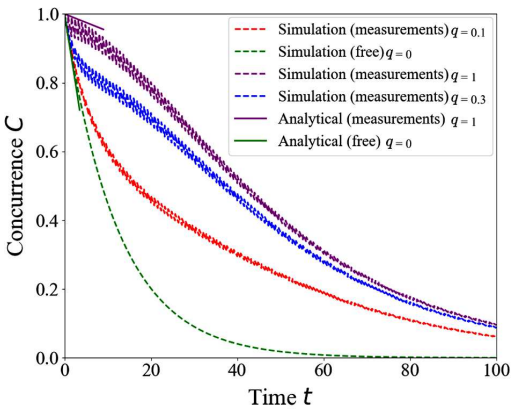

Fig. 4. (Color online) Time evolution of concurrence for a two-qubit entangled state under different scenarios. The lower curve represents the decay due solely to decoherence, following the analytic asymptotics Eq. (7). Overlaid on this, three upper curves illustrate how repeated joint measurements can preserve the entanglement; these curves correspond to different weak measurement forces (0.1, 0.3, and 1), and the under-measurement behavior is described by the analytic asymptotics Eq. (8). All parameters are the same as in Fig. 2

3.3. Influence of key parameters on the effectiveness of the method

In this subsection, we discuss the role of different parameters in the effectiveness of applying multiple joint weak measurements to mitigate the loss of coherence and entanglement.

The simulation consisted in solving the Lindblad master equation with Liouvillian (2) which describes the time evolution of the system density matrix ρ. The parameters of the Lindblad dynamics, namely the ratio of frequency detunings ω_2/ω_1, the relaxation rates γ_1 and γ_2, the dephasing rates $\gamma_{p1,2}$, the Planck number $\overline{n}$ indicating the role of temperature were freezed. The parameter of the weak measurements strength force q in Eq. (3) were varied systematically. The time evolution was integrated numerically using a second order Runge Kutta method with a fixed time step of $\Delta t = 0.01/\omega_1$. The total simulation time was $T_{\text{total}} = 100/\omega_1$. The time step was selected to ensure the stability and accuracy of the integration.

To evaluate the impact of measurement on the dynamics of the qubits two simulation protocols were employed. In the first protocol joint weak measurements on the subspace of Bell states $|\Psi^{\pm}\rangle$ were applied at regular intervals. In the second protocol no measurements were performed. In the first case, the measurement intervals were distributed evenly along the simulation timeline.

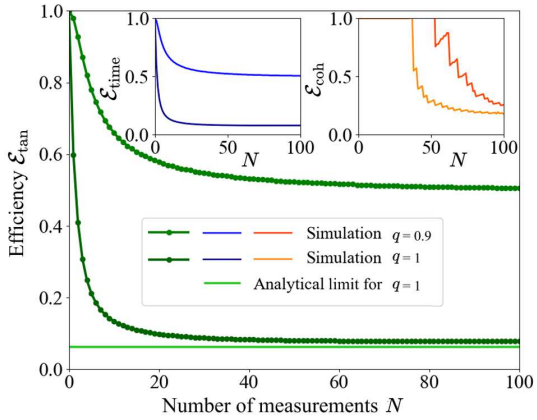

Fig. 5. (Color online) Dependence of three effectiveness characteristics, $\mathcal{E}_{\text{tan}}$, $\mathcal{E}_{\text{time}}$, and $\mathcal{E}_{\text{coh}}$, defined by Eqs. (9), (11), and (12), on the number of joint measurements performed during the interval $t = 100/\omega_1$. In addition to displaying analytic asymptotic behavior for the case with weak measurement force equal to 1, the plot features two curves corresponding to results of numeric calculations of weak measurement with forces of 0.9 and 1. One can see that even relatively infrequent joint weak measurements of the entangled qubit pair effectively suppress the loss of concurrence (as shown in the main panel and the first inset), as well as the degradation of the coherence measure C_{l_1} (presented in the second inset). Parameters are the same as for Fig. 2

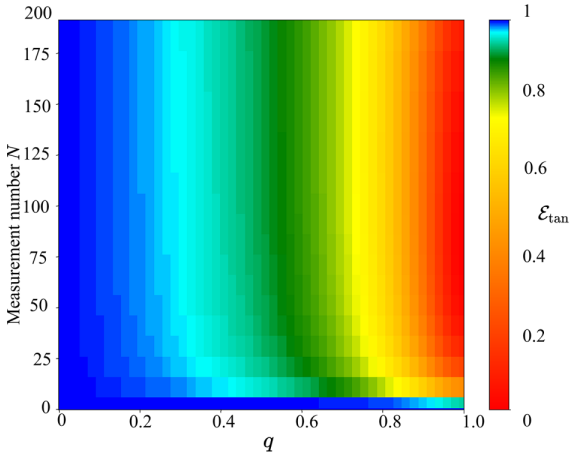

Fig. 6. (Color online) Dependence of the method effectiveness, as defined in Eq. (9), on the number of measurements N and the force parameter q of weak measurements. The color scale indicates the effectiveness

A rectangular grid of time points was used for sampling the elements of the density matrix and these values were stored at prescribed intervals to reduce computational overhead. After each integration step the density matrix was regularized to ensure that its trace remained normalized. For each simulation, the matrix elements of ρ were recorded and key metrics such as the concurrence and coherence measures were computed.

Figure 6 presents the results of the calculation of the effectiveness parameter $\mathcal{E}_{\text{tan}}$ for the different force parameter q and numbers N of joint weak measurements applied over the considered time interval.

The results indicate that the measurement frequency need not be very high and the effect is observed for $N \sim 50$. The Hamiltonian evolution determined by $\omega_{1,2}$ is suppressed in a manner analogous to the conventional Quantum Zeno Effect, but with the modification provided by the use of joint weak measurements. The force parameter q shows an influence on the effectiveness between 1.0 and 0.8, but decreases it on scale below 0.8.

4. Conclusions

An approach for suppressing the rate of loss of coherence and entanglement by applying multiple joint

weak measurements to an entangled system of qubits has been proposed. The standard Quantum Zeno Effect mitigates the Hamiltonian evolution by applying measurements at a sufficiently high frequency in order to freeze the evolution of the system interacting with its thermal bath. In contrast, the method presented here calculates the reduction in the rate of coherence loss for the non-Hamiltonian dynamics governed by the Lindblad equation and demonstrates the effectiveness of applying multiple joint weak measurements to the entangled system. This method is applicable in cases where the exact state to be preserved is not known, but information about the entanglement in the system is available. An example is provided by quantum algorithms in which a subset of qubits remains idle between the application of quantum gates.

1. M. Schlosshauer. Quantum Decoherence. *Phys. Rep.* **831**, 1 (2019).
2. G. Barenboim, A.M. Gago. Quantum decoherence effects: A complete treatment. *Phys. Rev. D* **110**, 095005 (2024).
3. J. Bordes, J.R. Brown, D.P. Watts, M. Bashkanov, K. Gibson, R. Newton, N. Zachariou. First detailed study of the quantum decoherence of entangled gamma photons. *Phys. Rev. Lett.* **133**, 132502 (2024).
4. L. Colmenárez, Z.-M. Huang, S. Diehl, M. Müller. Accurate optimal quantum error correction thresholds from coherent information. *Phys. Rev. Research* **6**, L042014 (2024).
5. K.J. Mei, W.R. Borrelli, A. Vong, B.J. Schwartz. Using machine learning to understand the causes of quantum decoherence in solution-phase bond-breaking reactions. *J. Phys. Chem. Lett.* **15** (4), 903 (2024).
6. T. Neidig, J. Rais, M. Bleicher, H. van Hees, C. Greiner. Open quantum systems with Kadanoff–Baym equations. *Phys. Lett. B* **851**, 138589 (2024).
7. Z. Ding, X. Li, L. Lin. Simulating open quantum systems using Hamiltonian simulations. *PRX Quantum* **5**, 020332 (2024).
8. D. Manzano. A short introduction to the Lindblad master equation. *AIP Adv.* **10** (2), 025106 (2020).
9. K. Kraus. General state changes in quantum theory. *Ann. Phys. (N.Y.)* **64**, 311 (1971).
10. B.M. Terhal. Quantum error correction for quantum memories. *Rev. Mod. Phys.* **87**, 307 (2015).
11. F.R.F. Pereira, S. Mancini, G.G. La Guardia. Stabilizer codes for open quantum systems. *Sci. Rep.* **13**, 10540 (2023).
12. B. Pokharel, N. Anand, B. Fortman, D.A. Lidar. Demonstration of fidelity improvement using dynamical decoupling with superconducting qubits. *Phys. Rev. Lett.* **121**, 220502 (2018).
13. C. Read, E. Serrano-Ensástiga, J. Martin. Platonic dynamical decoupling sequences for interacting spin systems. *Quantum* **9**, 1661 (2025).
14. N. Ezzell, B. Pokharel, L. Tewala, G. Quiroz, D.A. Lidar. Dynamical decoupling for superconducting qubits: A performance survey. *Phys. Rev. Appl.* **20**, 064027 (2023).
15. S. Dörscher, A. Al-Masoudi, M. Bober, R. Schwarz, R. Hobson, U. Sterr, C. Lisdat. Dynamical decoupling of laser phase noise in compound atomic clocks. *Commun. Phys.* **3**, 185 (2020).
16. I. Nodurft, A. Rodriguez Perez, N. Naimipour, G.C. Shaw. Suppressing polarization mode dispersion with the Quantum Zeno Effect. *Entropy* **27** (1), 27 (2025).
17. A. Streltsov, G. Adesso, M.B. Plenio. Colloquium: Quantum coherence as a resource. *Rev. Mod. Phys.* **89**, 041003 (2017).
18. C. Radhakrishnan, M. Parthasarathy, S. Jambulingam, T. Byrnes. Quantum coherence of the Heisenberg spin models with Dzyaloshinsky–Moriya interactions. *Sci. Rep.* **7**, 13865 (2017).
19. T. Baumgratz, M. Cramer, M. B. Plenio. Quantifying coherence. *Phys. Rev. Lett.* **113**, 140401 (2014).
20. R. Horodecki, P. Horodecki, M. Horodecki, K. Horodecki. Quantum entanglement. *Rev. Mod. Phys.* **81**, 865 (2009).
21. G. Vidal, R.F. Werner. Computable measure of entanglement. *Phys. Rev. A* **65**, 032314 (2002).
22. W.K. Wootters. Entanglement of formation of an arbitrary state of two qubits. *Phys. Rev. Lett.* **80**, 2245 (1998).

Received 02.05.25

О.М. Коноваленко, З.О. Майзеліс

МНОЖИННІ СЛАБКІ
СПІЛЬНІ ВИМІРЮВАННЯ ЯК СПОСІБ
ПРИГНІЧЕННЯ ДЕКОГЕРЕНЦІЇ

Множинні, рівномірно розподілені в часі, слабкі вимірювання застосовуються до двокубітної заплутаної системи, щоб зменшити швидкість її декогеренції, тобто не допустити зменшення недіагональних елементів. Схема подібна до квантового ефекту Зенона, але відрізняється частотою проведення вимірювань. Якщо в традиційному квантовому ефекті Зенона використовуються швидкі вимірювання для пригнічення гамільтонової динаміки, то запропонований метод використовує заплутаність між кубітами для зниження швидкості декогеренції. Продемонстровано, що це дозволяє частково пригнічувати декогеренцію в разі еволюції за рівнянням Ліндблада.

Ключові слова: спільні слабкі вимірювання, пригнічення декогеренції, квантовий ефект Зенона, еволюція за рівнянням Ліндблада.